$CdMoO_4$ synthesized by a microwave-assisted hydrothermal method and their photoluminescence and photocatality properties

Ana P. de Moura[1*], Larissa H. Oliveira[2], Camila S. Xavier[3], I.L.V.Rosa[2], Máximo Siu Li[4], Elson Longo[1], José A. Varela[1]

[1] Instituto de Química, UNESP ,CEP: 14800-900, Araraquara, SP – Brasil.
[2] Depto de Química, UFSCar, São Carlos – SP, Brasil
[3] Depto de Engenharia de Materiais, UFPel, Pelotas, RS – Brasil.
[4] Instituto de Física, USP, São Carlos, SP

ABSTRACT

In this work $CdMoO_4$ nanoparticles were obtained under hydrothermal conditions using microwave radiation (2.45 GHz) (MH) at 100 °C for different times. These powders were analyzed by X-ray diffraction (XRD), Field-emisson gum scanning electron microscopy (FEG-SEM), Ultraviolet-visible (UV-vis) absorption spectroscopy and photoluminescence (PL) measurements. XRD pattern confirmed that the pure $CdMoO_4$ phases were obtained. FEG-SEM powders present large-scale and homogeneous particles with microspheres-like morphology. UV-vis results were employed to determine the optical band gap these materials. Also, it showed existence of photoluminescence (PL) emission in the green wavelength range of 540-546 nm. Photocatalytic activity of $CdMoO_4$ nanocrystals was examined by monitoring the degradation of rhodamine B dye.

Keywords: cadmium molybdate, microwave-hydrothermal, photoluminescence, photocatality.

1 INTRODUCTION

As important materials, metal molybdates have received great research interest over the past few decades for their potential applications in various fields, such as photoluminescence [1], optical fibers [2], catalysis [3], humidity sensors[4], scintillators [5] magnetic properties [6], et al. Among them, cadmium molybdate ($CdMoO_4$), is one of the most important materials in optoelectronic areas due to its special electronic structures. However, to the best of our knowledge, there are only a few reports on $CdMoO_4$, whether on its synthesis process or properties. For example, $CdMoO_4$ powders with controlled shapes formed by a low-temperature hydrothermal method manifested a significantly different PL performance [7,8]. Cadmium molybdate (CdMoO4) is one of the metallic molybdate compounds with a scheelite structure, and has a body-center orthorhombic primitive cell with space group (*C64h*). Each site of Cd and Mo is surrounded by eight oxygen (octahedron) and four equivalent oxygen (tetrahedron) sites, respectively. The calculation of the electronic structure shows that the Cd *4d* state localizes at the bottom region of the O *2p* valence band, and the Cd *5s* state has a significant contribution to the bottom of the conduction band, composed of the Mo *4d* state [9,10] . Zhen et al. [11], Zhou et al. [12], and Wang et al.[13] reports the synthesis of CdMoO4 hollow microspheres composed of nanoparticles by an aqueous reaction process without using templates and additives. Recently, the microwave technology has been associated to the solvothermal process to accelerate the formation of molybdates with scheelite-type structure. The main advantages of the microwave-hydrothermal (MH) process are: (a) the kinetics of the reaction is enhanced by one to two orders of magnitude, (b) materials with different morphologies can be obtained, (c) rapid heating to treatment temperature saves time and energy and (d) reduced processing time. The present paper reports on the PL properties at room temperature of CdMoO4 powders processed in a domestic microwave-hydrothermal. The powders were characterized by X-ray diffraction (XRD), Fourier transform Raman spectroscopy, (FT-Raman), ultraviolet–visible (UV–vis) absorption spectroscopy and photoluminescence measurements.

2 EXPERIMENTAL SECTION

2.1 Synthesis of the Precursors

In a typical procedure, 2 mmol of sodium molybdate dihydrate (Na_2MoO_4. *x* $2H_2O$, 99.5%) solution was dissolved in 50 mL of distilled water. Then, 2mmol of such as cadmium (II) chlorite tetrahydrate ($Cd(NO_3)_2$. *x* $4H_2O$, 99.99%) was dissolved in 50 mL of deionized water which was slowly added to the sodium molybdate solution under magnetic stirring which produced a homogeneous solution (pH=7). The reaction mixture was transferred to a Teflon-lined stainless autoclave which was finally sealed and placed in the MH system using 2.45 GHz microwave radiation with maximum power of 800 W. MH conditions were kept at 100°C for 1, 2, 4, 8, 16 and 32 minutes. Then, the autoclave was naturally cooled to room temperature. These powders were water washed several times and then dried at 60°C for 8 h under atmospheric air in a conventional furnace.

2.2 Characterizantion

The obtained powders were structurally characterized by X-ray diffraction (XRD) using a Rigaku-DMax/2500PC with Cu K _ radiation (λ = 1.5406 A°) in the 2θ range from 10 to 75◦ with 0.02◦/min. Fourier transform Raman (FT-Raman) spectroscopy measurements were performed using a Bruker-RFS/100. The 1064 nm line of an Nd:YAG ion laser was used as excitation source, the power was kept at 55mW. The particle size of precursors and $CoMoO_4$ powders were determined using FE-SEM images and were calculated using the Image J. program. Ultraviolet–visible (UV–vis) spectroscopy for the spectra of optical reflectance of $CdMoO_4$ powders was taken using Cary 5G equipment. Photoluminescence (PL) measurements of the powders were taken with a U1000 Jobin-Yvon double monochromator coupled to a cooled GaAs photomultiplier and a conventional photon counting system. The 488.0 nm excitation wavelength of an argon ion laser was used. The photocatalytic activities were evaluated by the decomposition of rhodamine B (RhB) during irradiation with UV light (λ) 254 nm). Aqueous suspensions (usually 50 mL) of RhB (1×10^{-5} M) and $CdMoO_4$ powder 50 mg) were placed in a glass vessel. At given time intervals, 10 mL aliquots were sampled . Then the adsorption UV-vis spectrum of the
Filtrates was recorded using a UV-2550 (Shimadzu) spectrophotometer.

3 RESULTS AND DISCUSSION

3.1. X-ray diffraction analysis

Fig. 1 shows the XRD patterns of powders processed in MH at 100 ˚C for 1, 2, 4, 8, 16 and 32 minutes. All peaks can be perfectly indexed to a scheelite-type tetragonal structure with space group (*I41/a*), which is in accordance to the JCPDS card no. 07-0205. The peaks also indicate that the $CdMoO_4$ powders are free of secondary phases.

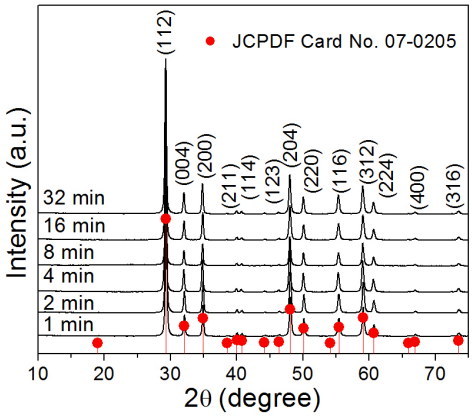

Figure 1: XRD patterns of $CdMoO_4$ powders processed by microwave-hydrothermal at 100 ◦C for different times. The vertical dashed lines indicate the position and relative intensity of JCPDS card no. 07-0205.

3.2. Fourier transform raman analysis

According to Basiev et al. [14], the vibrational modes in Raman spectra of molybdates are classified into two groups: internal and external ones. The internal vibrations are related to the $[MO_4]^{2-}$ molecular group with a stationary mass center. The external vibrations or lattice phonons are associated to the motion of the cation and the rigid molecular units. In the free space $[MO_4]^{2-}$ tetrahedrons presents *Td*-symmetry. In this case, the vibrations of the $[MO_4]^{2-}$ ions are constituted by four internal modes (ν_1 (A1), ν_2 (E), ν_3 (F2) and ν_4 (F2)), one free rotation mode (ν_{fr} (F1)) and one translation mode (F2). When the $[MO_4]^{2-}$ ions are present in a scheelite-type structure, its point symmetry reduces to *S4*. Therefore, all degenerative vibrations are split due to the crystal field effect. For a tetragonal scheelite primitive cell with $K = 0$ wavevector, the results estimated by the group-theory show the presence of 26 different types of vibrations, represented by Eq. (1)

$$\Gamma = 3Ag + 5Au + 5Bg + 3Bu + 5Eg + 5Eu \quad \text{(eq: 1)}$$

All the vibrations *A*g, *B*g and *E*g are Raman-active where 4 A_u and 4 E_u modes are active only in infrared frequencies. The system still includes the acoustic vibrations (1A_u and 1 E_u) and the silent modes (3 B_u) . Fig.2 shows the Raman spectra of $CdMoO_4$ produced by the microwave radiation method under different conditions.

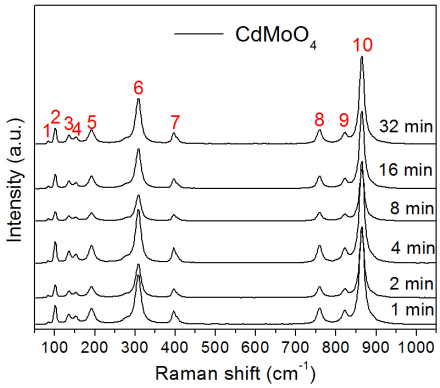

Figure 2: Raman spectra of $CdMoO_4$ powders processed by microwave hydrothermal at 100 ˚C for different times.

They show strong Raman peaks that indicate a strong interaction between the ions, which mainly arise from the stretching and bending vibrations of the shorter metal–oxygen bonds within the anionic groups. All Raman spectra were identified as n1(A_g), n3(B_g), n3(E_g), n4(E_g, B_g), and n2(A_g, B_g) at 864, 824, 760, 394,and 307cm^{-1}, respectively. Three rotation and two translation modes of $[MoO_4]^{2-}$ units were detected at 190,157,134, 98, and 81cm^{-1}, respectively [10]. These results are in accordance with those reported in the literature [15,16], and the little deviations of the vibration modes peak positions are due to the difference in geometries, particle sizes, and nature of the products.

3.3. Morphology and structure

Fig. 3 shows FE-SEM images of the powders. The $CdMoO_4$ powders present large-scale and homogeneous particles with microspheres-like morphology. All microspheres are aggregated with diameter of 70-110 nm and lengths ranging from 1.4 µm - 2.2µm.

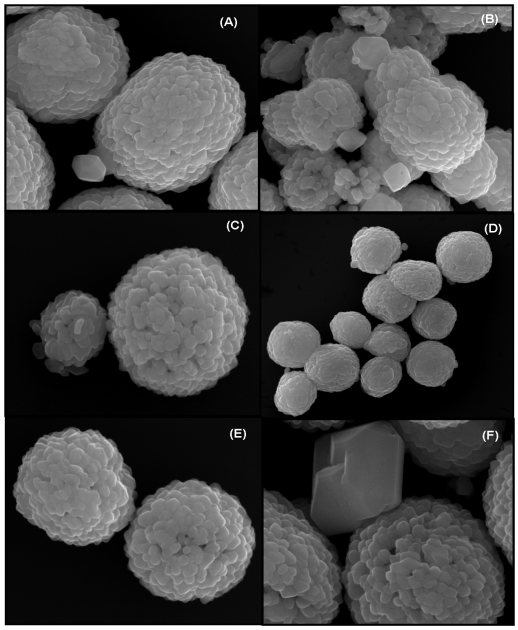

Figure 3: FE-SEM images of the $CdMoO_4$ *powders processed by microwave hydrothermal at 100 ˚C for different times 1min (A), 2 min (B), 4min(C), 8min (D), 16 min (E) and 32 min (F).*

Figure 4 (a) and (b) shows the average particle height distribution and average of particles diameters distribution for the $CdMoO_4$ powders processed at 100 ^{0}C for 1 min, respectively.

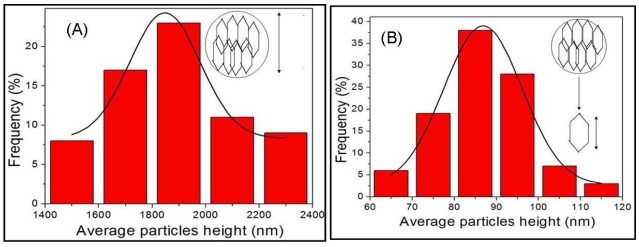

Figure 4: Average particle size distribution of $CdMoO_4$ powders processed in microwave-hydrothermal at 100 ^{o}C for 1min. (A)

3.4. Ultraviolet-visible absorption spectroscopy analysis

The optical band gap energy (*Eg*) of $CdMoO_4$ nanorods was estimated by the method proposed by Wood and Tauc[17]. According to these authors, the optical band gap energy is related with absorbance and photon energy by eq.(2):

$$h\upsilon\alpha \propto (h\upsilon - E_g)^2, \quad (eq:2)$$

where α is the absorbance, *h* is the Planck constant, *v* is the frequency and *E*g is the optical band gap. Therefore, the optical band gap was determined by extrapolation of the linear portion of the curve or tail. The band gap in the materials is related with absorbance and photon energy.

Therefore, the combination between absorbance and photoluminescence measurements allows discovering the energy levels in the materials and the optical band gap value. The E_{gap} values are presented in Table 1. The results obtained in this study are in accordance with the value of 3.2 eV already published [10]. The small difference in our results is probably due to particle size as well as the employed experimental procedure. Both effects promote different structural defects in the materials.

Table1: Gap Values of $CoMoO_4$ powders processed by microwave hydrothermal at 100 ^{o}C for different times.

Time (min)	*Gap values*
1 min	3.4 eV
2 min	3.3 eV
4 min	3.2 eV
8 min	3.5 eV
16mim	3.3 eV
32 min	3.4 eV

3.5. Photoluminescence emission analysis

Fig. 5 shows the PL emission spectra at room temperature of $CdMoO_4$ powders using an exciting wavelength of 488.0 nm. These PL spectra exhibited a broad band in the range of 400–700 nm which is ascribed to a multiphoton process where many intermediate levels of energy are involved in the PL process where relaxation occurs by several paths. The PL maximum emission intensity is related to the effects of structural order and disorder in the material which result in different electron transfer processes due to different distributions of intermediate levels of energy between the VB and CB. Studies of molybdates PL suggest that distorted clusters of $[MoO_3]$ and $[MoO_4]$ in the network lead to the formation of intermediate levels of energy within the band gap.

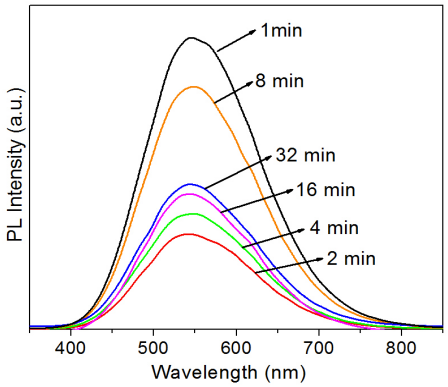

Figure 5: PL spectra of $CdMoO_4$ powders processed by microwave hydrothermal at 100 °C for different times

3.5. Photocatalytic activities

To investigate the potential applicability of the present $CdMoO_4$ particles for the removal of contaminants from wastewater, we evaluate their photocatalytic activity toward the photodegradation of rhodamine B (RhB) at room temperature as a test reaction. The synthesized sample 100 °C for 1 min selected for the test sample photocatalytic was obtained in shorter time and also showed that the best response photoluminescence.

Figure 6 shows the evolution of RhB absorption spectra in the presence of 50 mg of $CdMoO_4$ which we can see that the intensity of the absorption peaks corresponding to RhB diminishes slowly as the exposure time increases and completely disappears after 120 min. No new absorption bands appear in either the visible or ultraviolet regions, which indicate the complete photocatalytic degradation of RhB during the reaction.

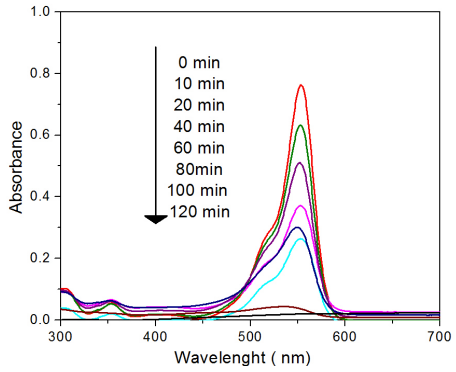

Figure 6: Absorption spectrum of a solution of RhB (1.0×10^{-5} M, 100 mL) in the presence of 50 mg of $CdMoO_4$

4 CONCLUSIONS

In summary, octaedros of the CdMoO4 nanostructures and microstructures were easily prepared. MAH method at a short time and a low temperature as compared to the conventional hydrothermal process. This method is very promising in the synthesis of other similar oxides and for industrial production because its preparation condition is simple and easy to control. XRD patterns and Raman spectra at room temperature showed that these powders have phases related to the $CdMoO_4$ with a space group of I41/a. all samples exhibit a PL emission maximum at ca. 540-546 nm (in the green emission) which indicates that the charge transference process as well as the trapping of electrons occurs because of a greater contribution of shallow holes rather than deep holes. The high photocatalytic activity of $CdMoO_4$ nanospheres are observed in the degradation of RhB under UV light irradiation.

5 ACKNOWLEDGEMENTS

The authors are grateful for the financial support of Brazilian agencies CAPES, CNPq and FAPESP.

REFERENCES

[1] P. Kozma, R. Bajgar, P. Kozma, Radiat. Phys. Chem., 65, 127, 2002;
[2] J. G. Rushbrooke and R. E. Ansorge, Nucl. Instrum. Methods Phys. Res., Sect. A, 280, 83, 1989
[3] S. Driscoll and U. S. Ozkan, Stud. Surf. Sci. Catal.,82, 367, 1994.
[4] W. Qu, W.Wlodarski and J. U. Meyer, Sens. Actuators,B, 64, 76, 2000.
[5] H. Wang, F. D. Medina, D. D. Liu and Y. D. Zhou, J. Phys.: Condens. Matter, 6, 5373, 1994;
[6] E. Ehrenberg, H. Weitzel, C. Heid, H. Fuess, G. Wltschek, T. Kroener, J. V. Tol and M. Bonnet, J. Phys.: Condens. Matter, 9, 3189, 1997.
[7] Yanfen Li, Shengwei Tan, Junying Jiang, Zaiyin Huang, Xuecai Tan, CrystEngComm, 2011, 13, 2649
[8] Y. Ren, J. F. Ma, Y. G. Wang, X. Y. Zhu, B. T. Lin, J. Liu, X. H. Jiang and J. T. Tao, J. Am. Ceram. Soc., 90,1251, 2007.
[9] H.Liu and L.Tan,Ionics,1657,2010.
[10] A.Phuruangrat, N. Ekthammathat, T.Thongtem, S.Thongtem, Journal of Physics and Chemistry of Solids 72, 176, 2011.
[11]L.Zhen,W.S.Wang,C.Y.Xu,W.Z.Shao,M.M.Ye,Z.L.Chen,ScriptaMater.58, 461, 2008.
[12]L.Zhou,W.Wang,H.Xu,S.Sun,Cryst.GrowthDes.8 3595, 2008.
[13]W.S.Wang,L.Zhen,C.Y.Xu,B.Y.Zhang,W.Z.Shao,J.Phys .Chem.B 110, 23154, 2006.
[14] T.T. Basiev, A.A. Sobol, Y.K. Voronko, P.G. Zverev, Opt. Mater. 15, 205, 2000.
[15] M.Daturi,G.Busca,M.M.Borel,A.Leclaire,P.Piaggio, J.Phys.Chem.B. 101, 4358, 1997.
[16] A.Jayaraman,S.Y.Wang,S.K.Sharma,Phys.Rev.B. 52, 9886, 1995.
[17] D.L. Wood, J. Tauc, Phys. Rev. B 5, 3144, 1972.